COMMUNICATIONS CHEMISTRY

ARTICLE

https://doi.org/10.1038/s42004-019-0110-y OPEN

Asymmetric total synthesis of rotenoids via organocatalyzed dynamic kinetic resolution

Saima Perveen[1], Shuang Yang[1,2,3], Miao Meng[4], Weici Xu[1], Guoxiang Zhang[1] & Xinqiang Fang[1,2,3]

Increasing effort has been made towards the asymmetric total synthesis of rotenoid natural products owing to their impressive biological and pharmaceutical activities. Here we report the modular asymmetric total synthesis of rotenoid natural products. The concise construction of the *cis*-fused tetrahydrochromeno[3,4-b]chromene core structure of rotenoids through N-heterocyclic carbene-catalyzed dynamic kinetic resolution is achieved, and a series of annulation products containing rotenoid key structures are rapidly assembled using this method. More importantly, the protocol enables the modular synthesis of a variety of rotenoid natural products in a highly convergent fashion, and the concise asymmetric total synthesis of tephrosin, the first asymmetric total synthesis of 12a-hydroxymunduserone, milletosin, and 12a-hydroxyrotenone, and the formal synthesis of deguelin are accomplished.

[1] State Key Laboratory of Structural Chemistry, Fujian Institute of Research on the Structure of Matter, 350100 Fuzhou, China. [2] Key Laboratory of Synthetic Chemistry of Natural Substances, Shanghai Institute of Organic Chemistry, 200032 Shanghai, China. [3] Center for Excellence in Molecular Synthesis, University of Chinese Academy of Sciences, 200032 Shanghai, China. [4] Department of Chemistry, Jinan University, 510632 Guangzhou, China. Correspondence and requests for materials should be addressed to X.F. (email: xqfang@fjirsm.ac.cn)

Rotenoids are an important class of natural products isolated from *Derris* and *Lonchocarpus* species and include a large amount of naturally occurred and structurally related compounds[1–3]. A *cis*-fused tetrahydrochromeno[3,4-b]chromene core (B and C rings) is featured by quite a lot of rotenoid compounds (Fig. 1), and a variety of biological and pharmacological properties including antibacterial, antiviral, antifungal, anticancer, antiplasmodial, anti-inflammatory, and insecticidal activities have been disclosed[4–10]. Particularly, 12a-hydroxymunduserone (**1a**) shows efficient antitumor activity for HepG2 proliferation[11]; tephrosin (**1b**) and deguelin (**1e**) are potent apoptotic and antiangiogenic reagents against various human cancer cells, such as lung, prostate, head and neck, and stomach cancer cells[12–15]; retenone (**1f**) and 12a-hydroxyrotenone (**1d**) have impressive inhibitory effect on breast cancer and lung cancer[16,17]; tephrosin (**1b**), milletosin (**1c**), and rotenone (**1f**) are also important pesticides[18,19].

Owing to the limited availability of these substances using the isolation method from the corresponding plants, chemical total synthesis of rotenoids has drawn long-term attention from both chemical and medicinal communities. However, to date most of the known reports are semi, formal, and racemic synthesis[20–27], and the successful methods of asymmetric total synthesis are still less developed. In this context, the Suh group reported a 12-step enantioselective total synthesis of deguelin (**1e**) using an iterative pyran-ring formation approach as the key step, and the overall yield of the target was 10.5% (Fig. 2a)[28]. Recently an elegant six-step (longest linear) synthesis of deguelin (**1e**) was achieved by the Scheidt group through a chiral thiourea-catalyzed cyclization strategy, and this represents the shortest route of deguelin synthesis (Fig. 2a)[29]. Starting from resorcine, de Konig and co-workers realized the total synthesis of rotenone (**1f**) in 2% total yield via 17 steps, and an alkyne-aldehyde coupling, a six-endo hydroarylation, and a Michael addition completed the key ring construction process (Fig. 2a)[30]. In contrast, the asymmetric total synthesis of hydroxyl group-substituted rotenoids, such as 12a-hydroxymunduserone (**1a**), tephrosin (**1b**), milletosin (**1c**), and 12a-hydroxyrotenone (**1d**), has been less achieved[31]. The report from the Winssinger group used chiral epoxide as starting material to produce the final target tephrosin (**1b**) in 7% yield via five key retro-synthetic steps and seven longest linear steps (Fig. 2a); noteworthy in this report is that deguelin (**1e**) could also be obtained via one more dehydroxylation step from tephrosin (**1b**)[32]. To the best of our knowledge, the enantioselective total synthesis of 12a-hydroxymunduserone (**1a**), milletosin (**1c**), 12a-hydroxyrotenone (**1d**), **1g**, and 12a-hydroxyisomillettone (**1h**) has not been accomplished (Fig. 1).

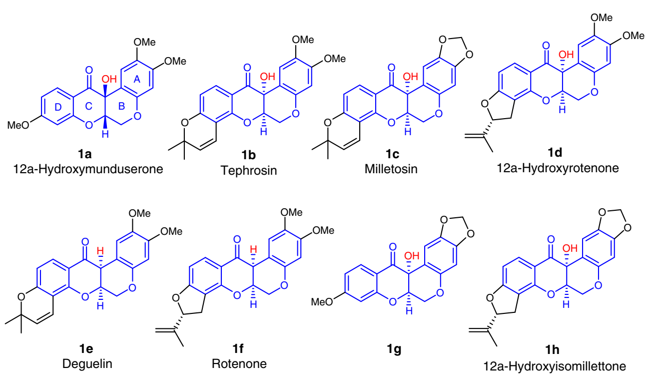

Fig. 1 Selected rotenoid natural products with *cis*-fused core structures. The blue color indicates the same core structure of many rotenoid natural products, and the red atoms show the different substituents of the core structure

Here we describe a synthetic plan that can not only lead to the concise synthesis of a specific rotenoid natural product, but also can be used as a general approach to rapidly produce a large amount of compounds that belong to rotenoid family. A careful evaluation of the structure of **1a**−**1f** and other rotenoid compounds reveals that, besides the core bicyclic ring structure (B and C rings), in many cases, they share the same substituted A ring and D ring. For instance, the methoxy-substituted D ring of **1a** also exists in **1g**; a cyclohexenyl ether structure is found in **1b**, **1c**, and **1e**; moreover, a chiral benzocyclopentane unit appears in **1d**, **1f**, and **1h**. On the other side, two methoxy groups at A ring exist in **1a**, **1b**, **1d**, **1e**, and **1f**; a 1,3-dioxolane moiety occurs in **1c**, **1h**, and **1g** (Fig. 1). These features lead us to the idea that if these natural products can be divided into two pieces (modules), the combination of different pieces will lead to different natural products, thus simplifying the total synthesis of rotenoid family natural products. To make the plan possible, a two-step key retrosynthesis route is proposed and shown in Fig. 2b. The route features first the dynamic kinetic resolution (DKR)-mediated C-C bond formation via asymmetric benzoin reaction, a powerful transformation pioneered by Enders and Suzuki[33–43], and then the forge of C-O bond via an S_N2 reaction. This plan leads to two units of acetal/aldehyde modules (i.e., **A1**, **A2**, and **A3**) and ketone modules (i.e., **B1** and **B2**) (Fig. 2c). Then as mentioned above, the combination of **A1** and **B1** will construct **1a** (12a-hydroxymunduserone), and similarly, **A2** and **B1** will lead to **1b** (tephrosin), **A2** together with **B2** will get **1c** (milletosin), and so on. Furthermore, using Winssinger's dehydration method, **1e** (deguelin) can be produced from **1b**, and **1f** (rotenone) can be obtained from **1d**. Thus, a large amount of rotenoid type natural products with *cis*-fused bicyclic core skeletons can be concisely and systematically synthesized using this approach.

Results

Optimization of the reaction conditions. Apparently, the efficiency and stereoselectivities of NHC-catalyzed DKR step are critical for the success of the whole research project. In recent years, the kinetic resolutions of a series of racemates have been achieved via NHC organocatalysis[44–48]. Particularly, the elegance of NHC-catalyzed DKR processes have been demonstrated by the Scheidt, Johnson, Wang, Chi, Fang, and Biju groups, respectively[49–58]. Therefore, to test our hypothesis, we selected racemic **2a** as model substrate for further studies (Fig. 3). However, as outlined in Table 1, the optimization of reaction conditions proved a significant challenge mainly arising from the formation of a series of by-products and the enantioselectivity control of the desired benzoin product. For instance, the reaction of **3a** under the catalysis of **A**[59–62] using KOH as the base in THF afforded the desired product **3a** in 54% yield with high diastereoselectivity; however, poor enantioselectivity was observed and significant amount of aldol product **3aa** was obtained (Table 1, entry 1). Replacing KOH with Et_3N or Na_2CO_3 increased the yield of **3a** to an excellent level, but still with low er values (Table 1, entries 2−3). To our delight, decreasing the temperature showed beneficial effect on the reaction (Table 1, entry 4), and catalyst **B**[59–62] led to a promising 75:25 er of **3a**, albeit in a low yield (Table 1, entry 5), and in both cases the formation of **3aa** could not be suppressed. Catechol type additives have proved useful for enhancing the stereoselectivities of NHC-catalyzed reactions by Rovis, Chi, and Fang's works[63–66]; therefore, we tested the reaction by introducing additive **a1**. We were pleased to find that the annulation product **3a** was obtained in excellent 90% yield with 83:17 er (Table 1, entry 6). Additive **a2** also displayed promotion effect on the results (Table 1, entry 7). Slight promotions of the enantioselectivity were also observed when **a3** or **a4** was used

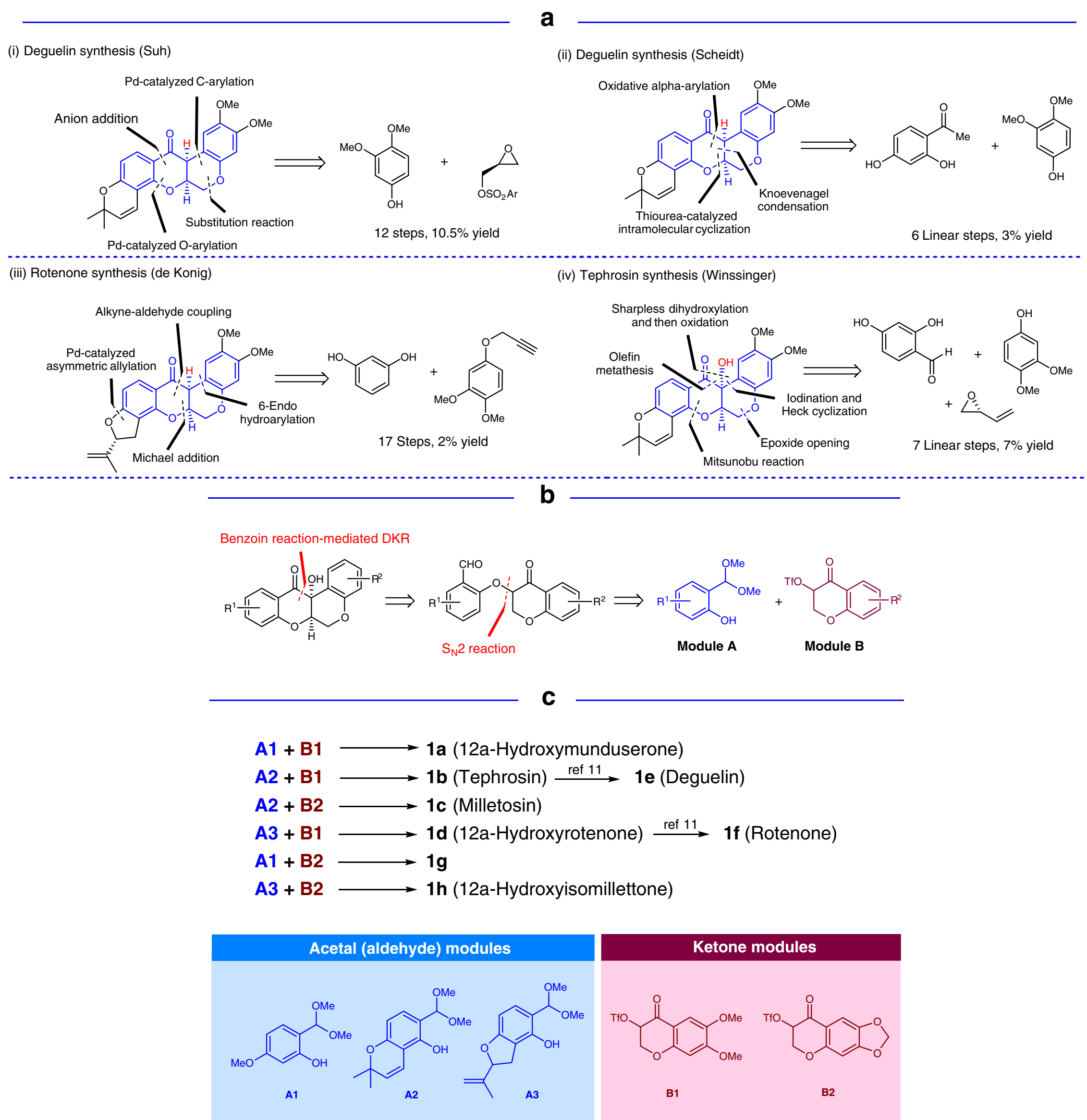

Fig. 2 Selected known synthetic routes and our synthetic plan. **a** Selected asymmetric total syntheses of rotenoid natural products. **b** Our two-step key retro-synthetic plan. **c** Modular synthesis of rotenoid natural products

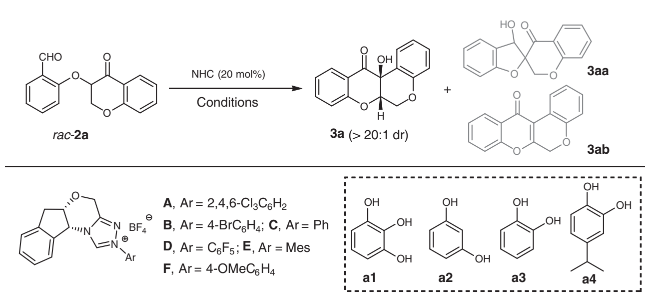

Fig. 3 Model system used for reaction optimization. Conditions used for optimization of the catalyst, base, additive, solvent, and temperature can be found in Table 1

(78:22 er, 22% yield for **a3**, and 76:24 er, 44% yield for **a4**, respectively). Then we found that the use of both **a1** and **a2** resulted in the formation of **3a** with good 90.5:9.5 er, together with small amount of the aldol product (Table 1, entry 8). Under the same conditions, we then surveyed catalysts **A**, **C**, **D**, **E**, and **F**[59], but unfortunately, no better results were detected (Table 1, entries 9–13). Gladly, we found that the addition of the third additive **a3** or **a4** and simultaneously increasing the amount of the base could slightly increase the enantioselectivity of the reaction, although one more side product **3ab**, formed probably via the dihydroxylation from **3a**, was also detected (Table 1, entries 14–15); therefore, we checked the reaction using additives **a1**–**a4**, and 93.5:6.5 er of **3a** was obtained (Table 1, entry 16). Although the exact role of catechol type additives remains unambiguous, we believe that the hydrogen-bonding network between the OH groups of catechol type additives, the carbonyl groups of substrates, and the OH groups of Breslow intermediates plays a vital role in enhancing the stereoselectivity of the reaction[63–66]. Variation of the solvent using toluene proved not beneficial to the reaction (Table 1, entry 17), but CH_3CN allowed access to **3a** with excellent 95:5 er in 60% yield (Table 1, etnry 18). Under these conditions, using Et_3N instead of KOH further increased the enantioselectivity of the reaction, but **3a** was isolated in only 30% yield (Table 1, entry 19). To our delight, the use of Cs_2CO_3 allowed the formation of **3a** in good 73% yield with

Table 1 Reaction condition optimization[a]

Entry	Cat.	Base (equiv), additive, solvent, temp	Yield (3a/3aa/3ab, %)	er (3a, %)
1	**A**	KOH (0.8), THF, rt	54/37/0	52:48
2	**A**	Et_3N (0.8), THF, rt	90/0/0	55:45
3	**A**	Na_2CO_3 (0.8), THF, rt	95/0/0	56:44
4	**A**	KOH (0.8), THF, −20 °C	43/32/9	68:32
5	**B**	KOH (0.8), THF, −20 °C	20/63/0	75:25
6	**B**	KOH (0.8), **a1**, THF, −20 °C	90/0/0	83:17
7	**B**	KOH (0.8), **a2**, THF, −20 °C	87/5/0	80:20
8	**B**	KOH (0.8), **a1**/**a2**, THF, −20 °C	68/12/0	90.5:9.5
9	**A**	KOH (0.8), **a1**/**a2**, THF, −20 °C	44/32/0	82.5:17.5
10	**C**	KOH (0.8), **a1**/**a2**, THF, −20 °C	34/47/0	85:15
11	**D**	KOH (0.8), **a1**/**a2**, THF, −20 °C	Trace	-
12	**E**	KOH (0.8), **a1**/**a2**, THF, −20 °C	Trace	-
13	**F**	KOH (0.8), **a1**/**a2**, THF, −20 °C	35/48/0	84:16
14	**B**	KOH (1.5), **a1**/**a2**/**a3**, THF, −20 °C	63/21/10	91:9
15	**B**	KOH (1.5), **a1**/**a2**/**a4**, THF, −20 °C	67/12/9	92.5:7.5
16	**B**	KOH (1.5), **a1**/**a2**/**a3**/**a4**, THF, −20 °C	79/11/9	93.5:6.5
17	**B**	KOH (1.5), **a1**/**a2**/**a3**/**a4**, toluene, −20 °C	70/11/8	80.5:19.5
18	**B**	KOH (1.5), **a1**/**a2**/**a3**/**a4**, CH_3CN, −20 °C	60/13/10	95:5
19	**B**	Et_3N(1.5), **a1**/**a2**/**a3**/**a4**, CH_3CN, −20 °C	30/34/10	96.5:3.5
20	**B**	Cs_2CO_3 (1.5), **a1**/**a2**/**a3**/**a4**, CH_3CN, −20 °C	**73/7/4**	**97:3**

[a]Reaction conditions: **2a** (0.1 mmol), NHC (20 mol%), solvent (1 mL), 0.5 equiv for each additive, argon protection. All isolated yields were based on **2a**. All ee values were determined via HPLC analysis on a chiral stationary phase.

excellent 97:3 er (Table 1, entry 20). Further conditions screening did not lead to better results and therefore the conditions listed in entry 20 (Table 1) were set as the optimal ones.

Synthesis of rotenoid analogues via dynamic kinetic resolution. Having found the suitable conditions for our plan using the model reaction, we then further evaluated the substrate scope and limitation of this NHC-catalyzed DKR process to evaluate the synthetic potential of producing rotenoid analogues. Pleasingly, different substituents and substitution patterns on the both aryl rings having electron-withdrawing and electron-donating groups were all tolerated (Fig. 4). For instance, introduction of electron-withdrawing Cl, Br, or F group into the formyl aryl units of substrates showed little effect on the outcomes, delivering the corresponding products in good yields with up to 94.5:5.5 er (Figs. 4, 3b–d). Similarly, substrates equipped with electron-donating Me or OMe group at the aromatic aldehyde moieties performed well, allowing access to **3e** and **3f** with 91:9 and 96:4 er, respectively (Figs. 4, 3e, f). Substrate diversity was further evaluated by the installation of substituents into both formyl aryl rings and aromatic ketones. To our delight, when R^1 was electron-donating Me and R^2 was electron-withdrawing Cl group, the reaction occurred smoothly, with **3k** obtained in 77% yield with 94:6 er (Figs. 4, 3k). Moreover, the combinations of electron-withdrawing R^1 such as Cl or Br with electron-donating R^2 such as OMe were also tolerated under the optimal conditions, with good er values gotten for **3l** and **3m** (Figs. 4, 3l, m). Finally, dimethyl-substituted substrate **2n** was also tested, and the corresponding product **3n** was formed in 71% yield with 93.5:6.5 er (Figs. 4, 3n). The absolute configuration of the annulation products was determined via the X-ray single crystal structure analysis of **3b** (Supplementary Data 1 and Supplementary Table 1), and the *cis*-fused bicyclic ring skeleton was unambiguously confirmed.

Synthesis of related natural products via dynamic kinetic resolution. Having successfully developed a protocol for the rapid asymmetric construction of the rotenoid core structure and evaluated the generality of this method, we then commenced to

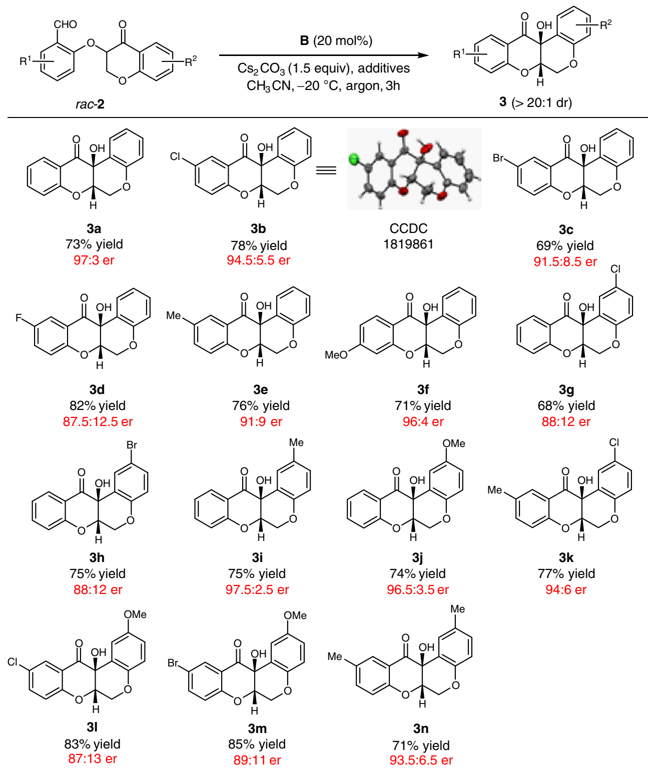

Fig. 4 Substrate scope. Reaction conditions: **2** (0.1 mmol), NHC (20 mol%), Cs_2CO_3 (1.5 equiv), **a1** (0.5 equiv), **a2** (0.5 equiv), **a3** (0.5 equiv), **a4** (0.5 equiv), CH_3CN (1 mL), argon protection

test its power in the modular total synthesis of related natural products. 12a-Hydroxymunduserone (**1a**), tephrosin (**1b**), milletosin (**1c**), and 12a-hydroxyrotenone (**1d**) were selected for further investigation. As has been demonstrated in Fig. 2c, these natural products can be derived from three aldehyde modules (**A1**, **A2**, and **A3**) and two ketone modules (**B1** and **B2**). So at the

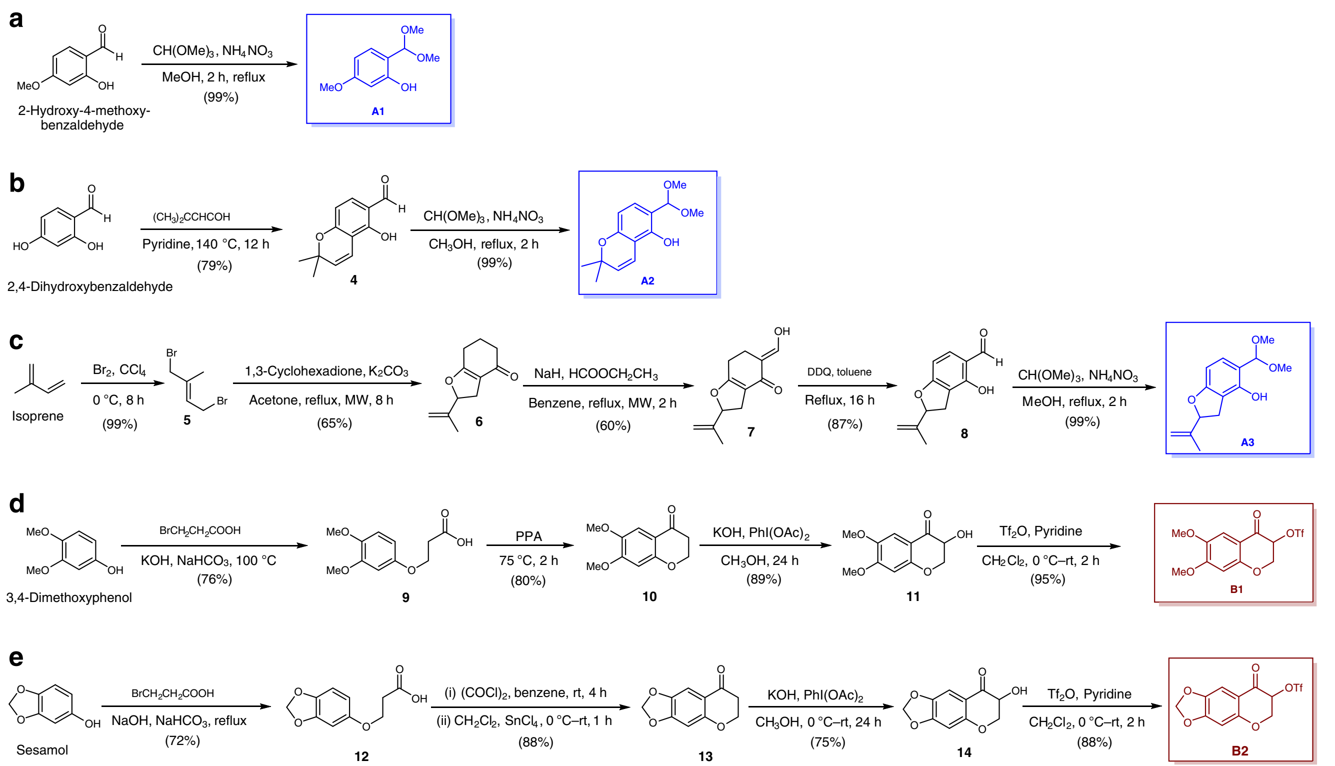

Fig. 5 Synthesis of aldehyde modules and ketone modules. **a** Synthesis of module **A1**. **b** Synthesis of module **A2**. **c** Synthesis of module **A3**. **d** Synthesis of module **B1**. **e** Synthesis of module **B2**

first stage we need to get all modules ready for the synthesis of the final natural products. As listed in Fig. 5a, **A1** could be easily obtained via one-step protection from commercially available 2-hydroxy-4-methoxybenzaldehyde in quantitative yield. Furthermore, **A2** was synthesized from 2,4-dihydroxybenzaldehyde via a two-step method (Fig. 5b). To simplify the synthesis of **A3**, we envisioned the making of **A3** in its racemic form, and the later DKR process would produce the corresponding chiral natural product **1d** in a stereodivergent fashion together with its epimer. Thus, the bromination of isoprene led to dibromide **5**, and the following annulation with 1,3-cyclohexadione afforded cyclic enone **6**. Reaction of **6** with ethyl formate with the assistance of microwave and the subsequent oxidation delivered hydroxybenzaldehyde **8**. Then after protection **A3** was gotten in 33% total yield (Fig. 5c).

Then the second stage is to make ketone modules **B1** and **B2**. Starting from 3,4-dimethoxyphenol, acid **9** was formed in 76% yield via substitution. Then the PPA-catalyzed Friedel-Crafts reaction afforded ketone **10**, and after α-hydroxylation, **11** was generated. Protection of **11** using Tf_2O provided **B1** in 89% yield (Fig. 5d). Using the similar method, module **B2** could also be furnished in 48% total yield from sesamol (Fig. 5e).

Having gotten all modules in hand, we could carry out the final stage to make natural products **1a**−**1d**. To our delight, and as illustrated in Fig. 6a, the S_N2 reaction between **A1** and **B1** allowed the smooth conjunction of two modules through C-O bond formation, then after deprotection, *rac*-**15** was liberated. The NHC-catalyzed intramolecular annulation of *rac*-**15** under the standard conditions proceeded smoothly, affording natural product 12a-Hydroxymunduserone (**1a**) in 58% isolated yield with 95.5:4.5 er (7 linear steps, 21% overall yield). Subsequently, the final total synthesis of tephrosin (**1b**) was achieved through the combination of **A2** and **B1**, followed by the DKR-mediated annulation under slightly modified conditions (86.5:13.5 er, seven linear steps, 28% overall yield) (Fig. 6b). Similarly, the merger of **A2** and **B2** produced *rac*-**17**, which could undergo smooth C−C bond formation to release milletosin (**1c**) in 60% yield with 94.5:5.5 er (eight linear steps, 24% overall yield) (Fig. 6c). To our pleasure, 12a-hydroxyrotenone (**1d**) could also be obtained using this modular synthetic method with 99:1 er (8 linear steps, 10% overall yield), together with its separable epimer (Fig. 6d). We found that recrystallization could be used to further increase the er values of the products (Fig. 6b, c). It's also worthwhile to mention that using Winssinger's dehydroxylation method[32], the formal synthesis of **1e** (deguelin) could also be realized from **1b**. Compared to the prior arts of rotenoid asymmetric total synthesis[28–32], this strategy can achieve the target molecules using comparable or less steps, and can dramatically improve the total yields of the corresponding natural products. More importantly, this method could render the modular synthesis of a variety of rotenoid natural products using a systematic approach, which will absolutely improve the efficiency of producing these biologically important substances and assist the related medicinal research.

Discussion

In summary, we have successfully developed an N-heterocyclic carbene-catalyzed dynamic kinetic resolution process to achieve the rapid construction of rotenoid *cis*-fused tetrahydrochromeno [3,4-b]chromene core structures, and the method was proved compatible to a series of substituents with different electronic properties. More importantly, this protocol could enable the production of various rotenoid natural products via a systematic and modular approach. Using this strategy, we accomplished the concise total synthsis of tephrosin, the first enantioselective total synthesis of 12a-hydroxymunduserone, milletosin, and 12a-hydroxyrotenone, and the formal synthesis of deguelin.

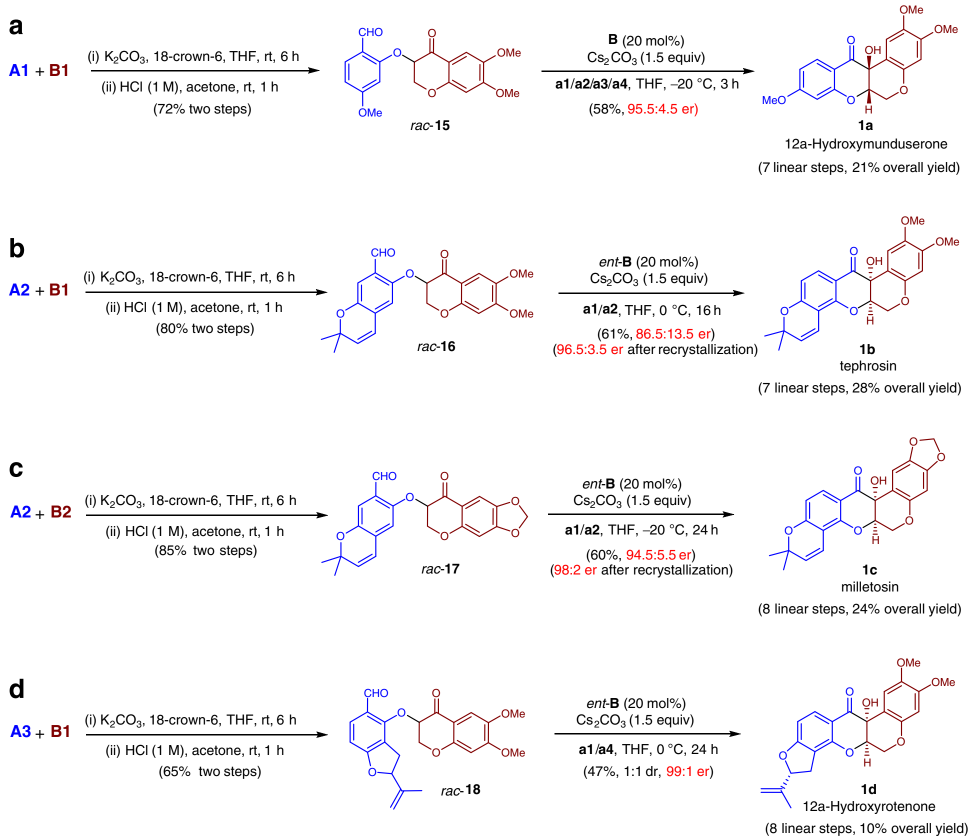

Fig. 6 Total synthesis of rotenoid nature products. **a** Synthesis of 12a-hydroxymunduserone (**1a**). **b** Synthesis of tephrosin (**1b**). **c** Synthesis of milletosin (**1c**). **d** Synthesis of 12a-hydroxyrotenone (**1d**)

Methods

Typical procedure for the preparation of substrate. See Supplementary Methods and Supplementary Figure 1.

Typical procedure for the benzoin reaction. See Supplementary Methods and Supplementary Figure 2.

Total synthesis of natural product 12a-hydroxymunduserone (1a). See Supplementary Methods, Supplementary Figure 3 and Supplementary Table 2.

Total synthesis of natural product tephrosin (1b). See Supplementary Methods, Supplementary Figures 4–6 and Supplementary Table 3.

Total synthesis of natural product milletosin (1c). See Supplementary Methods, Supplementary Figures 7–9 and Supplementary Table 4.

Total synthesis of natural product 12a-hydroxyrotenone (1d). See Supplementary Methods, Supplementary Figures 10–12 and Supplementary Table 5.

^{1}H NMR and ^{13}C NMR spectra of substrates and products. See Supplementary Figures 13–40.

HPLC spectra of products. See Supplementary Figures 41–54.

^{1}H NMR and ^{13}C NMR spectra of synthetic natural products. See Supplementary Figures 55–71.

HPLC spectra of synthetic natural products. See Supplementary Figures 71–77.

Crystallography. The CIF for compound **3b** is available in Supplementary Data 1. Crystal data and structure refinement are shown in Supplementary Table 1.

Data availability

Data for the crystal structures reported in this paper have been deposited at the Cambridge Crystallographic Data Centre (CCDC) under the deposition numbers CCDC 1819861. Copies of these data can be obtained free of charge via www.ccdc.cam.ac.uk/data_request/cif. All other data supporting the findings of this study, including compound characterization, are available within the paper and its Supplementary Information files, or from the corresponding authors on request.

Received: 16 October 2018 Accepted: 11 December 2018
Published online: 25 January 2019

References

1. Gerhäuser, C. et al. Rotenoids mediate potent cancer chemopreventive activity through transcriptional regulation of ornithine decarboxylase. *Nat. Med.* **1**, 260–266 (1995).
2. Santos, R. A., David, J. M. & David, J. P. Detection and quantification of rotenoids from *Clitoria fairchildiana* and its lipids profile. *Nat. Prod. Commun.* **11**, 631–632 (2016).
3. Deyou, T. et al. Rotenoids, flavonoids, and chalcones from the root bark of *Millettia usaramensis*. *J. Nat. Prod.* **78**, 2932–2939 (2015).
4. Takashima, J., Chiba, N., Yoneda, K. & Ohsaki, A. Derrisin, a new rotenoid from *Derris malaccensis* plain and anti-*helicobacter pylori* activity of its related constituents. *J. Nat. Prod.* **65**, 611–613 (2002).
5. Phrutivorapongkul, A., Lipipun, V., Ruangrungsi, N., Watanabe, T. & Ishikawa, T. Studies on the constituents of seeds of *Pachyrrhizus erosus* and their anti-herpes simplex virus (HSV) activities. *Chem. Pharm. Bull.* **50**, 534–537 (2002).
6. Yang, S. W. et al. Three new phenolic compounds from a manipulated plant cell culture. *J. Nat. Prod.* **64**, 313–317 (2001).
7. Fang, N. & Casida, J. E. Anticancer action of cubé insecticide: correlation for rotenoid constituents between inhibition of NADH: ubiquinone oxidoreductase and induced ornithine decarboxylase activities. *Proc. Natl Acad. Sci. USA* **95**, 3380–3384 (1998).

8. Yenesew, A. et al. Anti-plasmodial activities and X-ray crystal structures of rotenoids from *Millettia usaramensis* subspecies *usaramensis*. *Phytochemistry* **64**, 773–779 (2003).
9. Mathias, L., Silva, B. P. D., Mors, W. B. & Parente, J. P. Isolation and structural elucidation of a novel rotenoid from the seeds of *Clitoria fairchildiana*. *Nat. Prod. Res.* **19**, 325–329 (2005).
10. Fang, N. & Casida, J. E. New bioactive flavonoids and stilbenes in cubé resin insecticide. *J. Nat. Prod.* **62**, 205–210 (1999).
11. Wu, X. et al. 12a-Hydroxymunduserone induces apoptosis of human hepatocarcinoma cells through Wnt/β-catenin pathway. *Genom. Appl. Biol.* **35**, 1881–1886 (2016).
12. Luyengi, L. et al. Rotenoids and chalcones from *Mundulea sericea* that inhibit phorbol ester-induced ornithine decarboxylase activity. *Phytochemistry* **36**, 1523–1526 (1994).
13. Garcia, J., Barluenga, S., Gorska, K., Sasse, F. & Winssinger, N. Synthesis of deguelin-biotin conjugates and investigation into deguelin's interactions. *Bioorg. Med. Chem.* **20**, 672–680 (2012).
14. Ye, H. et al. Cytotoxic and apoptotic effects of constituents from *Millettia pachycarpa* benth. *Fitoterapia* **83**, 1402–1408 (2012).
15. Matsuda, H. et al. Rotenoids and flavonoids with anti-invasion of HT1080, anti-proliferation of U937, and differentiation-inducing activity in HL-60 from *Erycibe expansa*. *Bioorg. Med. Chem.* **15**, 1539–1546 (2007).
16. Cheenpracha, S., Karalai, C., Ponglimanont, C. & Chantrapromma, K. Cytotoxic rotenoloids from the stems of *Derris trifoliate*. *Can. J. Chem.* **85**, 1019–1022 (2007).
17. Leuner, O. et al. Cytotoxic constituents of Pachyrhizus tuberosus from Peruvian amazon. *Nat. Prod. Commun.* **8**, 1423–1426 (2013).
18. Puyvelde, L. V. et al. Isolation and structural elucidation of potentially insecticidal and acaricidal isoflavone-type compounds from *Neorautanenia mitis*. *J. Nat. Prod.* **50**, 349–356 (1987).
19. Belofsky, G. et al. Antimicrobial and antiinsectan phenolic metabolites of *Dalea searlsiae*. *J. Nat. Prod.* **77**, 1140–1149 (2014).
20. Anzeveno, P. B. Rotenoid interconversion. Synthesis of deguelin from rotenone. *J. Org. Chem.* **44**, 2578–2580 (1979).
21. Fukami, H., Oda, J., Nakajima, M. & Sakata, G. Total synthesis of dl-deguelin. *Agric. Biol. Chem.* **25**, 252–253 (1961).
22. Fukami, H., Oda, J., Sakata, G. & Nakajima, M. Total synthesis of dl-deguelin. *Bull. Agric. Chem. Soc. Jpn.* **24**, 327–328 (1960).
23. Omokawa, H. & Yamashita, K. Synthesis of (±)-deguelin. *Agric. Biol. Chem.* **38**, 1731–1734 (1974).
24. Pastine, S. J. & Sames, D. Concise synthesis of the chemopreventitive agent (±)-deguelin via a key 6-endo hydroarylation. *Org. Lett.* **5**, 4053–4055 (2003).
25. Granados-Covarrubias, E. H. & Maldonado, L. A. Protected cyanohydrins in the synthesis of rotenoids: (±)-munduserone and (±)-cis-12a-hydroxymunduserone. *J. Org. Chem.* **74**, 5097–5099 (2009).
26. Xu, S. et al. Concise total synthesis of (±)-deguelin and (±)-tephrosin using a vinyl iodide as a key building block. *J. Nat. Prod.* **81**, 1055–1059 (2018).
27. Miyano, M. Rotenoids. XX.[1] Total synthesis of rotenone. *J. Am. Chem. Soc.* **87**, 3958–3962 (1965).
28. Lee, S. et al. Total synthesis of (–)-deguelin via an iterative pyran-ring formation strategy. *Chem. Commun.* **51**, 9026–9029 (2015).
29. Farmer, R. L. & Scheidt, K. A. A Concise enantioselective synthesis and cytotoxic evaluation of the anticancer rotenoid deguelin enabled by a tandem Knoevenagel/conjugate addition/decarboxylation sequence. *Chem. Sci.* **4**, 3304–3309 (2013).
30. Georgiou, K. H., Pelly, S. C. & de Koning, C. B. The first stereoselective synthesis of the natural product, rotenone. *Tetrahedron* **73**, 853–858 (2017).
31. Khorphueng, P., Tummatorn, J., Petsom, A., Taylor, R. J. K. & Roengsumran, S. Total synthesis of 6-deoxyclitoriacetal isolated from *Stemona collinsae* Craib. *Tetrahedron Lett.* **47**, 5989–5991 (2006).
32. Garcia, J., Barluenga, S., Beebe, K., Neckers, L. & Winssinger, N. Concise modular asymmetric synthesis of deguelin, tephrosin and investigation into their mode of action. *Chem. Eur. J.* **16**, 9767–9771 (2010).
33. Enders, D., Niemeier, O. & Henseler, A. Organocatalysis by N-heterocyclic carbenes. *Chem. Rev.* **107**, 5606–5655 (2007).
34. Izquierdo, J., Hutson, G. E., Cohen, D. T. & Scheidt, K. A. A continuum of progress: applications of N-hetereocyclic carbene catalysis in total synthesis. *Angew. Chem., Int. Ed.* **51**, 11686–11698 (2012).
35. Hopkinson, M. N., Richter, C., Schedler, M. & Glorius, F. An overview of N-heterocyclic carbenes. *Nature* **510**, 485–496 (2014).
36. Flanigan, D. M., Romanov-Michailidis, F., White, N. A. & Rovis, T. Organocatalytic reactions enabled by N-heterocyclic carbenes. *Chem. Rev.* **115**, 9307–9387 (2015).
37. Enders, D. & Balensiefer, T. Nucleophilic carbenes in asymmetric organocatalysis. *Acc. Chem. Res.* **37**, 534–541 (2004).
38. Johnson, J. S. Catalyzed reactions of acyl anion equivalents. *Angew. Chem. Int. Ed. Engl.* **43**, 1326–1328 (2004).
39. Moore, J. L. & Rovis, T. Carbene catalysts. *Top. Curr. Chem.* **291**, 77–144 (2010).
40. Biju, A. T., Kuhl, N. & Glorius, F. Extending NHC-catalysis: coupling aldehydes with unconventional reaction partners. *Acc. Chem. Res.* **44**, 1182–1195 (2011).
41. Enders, D., Niemeier, O. & Raabe, G. Asymmetric synthesis of chromanones via N-heterocyclic carbene catalyzed intramolecular crossed-benzoin reactions. *Synlett* 2431–2434 (2006).
42. Takikawa, H. & Suzuki, K. Modified chiral triazolium salts for enantioselective benzoin cyclization of enolizable keto-aldehydes: synthesis of (+)-sappanone B. *Org. Lett.* **9**, 2713–2716 (2007).
43. Vora, H. U. & Rovis, T. Asymmetric N-heterocyclic carbene (NHC) catalyzed acyl anion reactions. *Aldrichimica Acta* **44**, 3–11 (2011).
44. Bugaut, X. & Glorius, F. Organocatalytic umpolung: N-heterocyclic carbenes and beyond. *Chem. Soc. Rev.* **41**, 3511–3522 (2012).
45. Menon, R. S., Biju, A. T. & Nair, V. Recent advances in N-heterocyclic carbene (NHC)-catalysed benzoin reactions. *Beilstein J. Org. Chem.* **12**, 444–461 (2016).
46. Yang, S. & Fang, X. Kinetic resolutions enabled by N-heterocyclic carbene catalysis. *Curr. Org. Synth.* **14**, 654–664 (2017).
47. Lu, S., Poh, S. B., Siau, W.-Y. & Zhao, Y. Kinetic resolution of tertiary alcohols: highly enantioselective access to 3-hydroxy-3-substituted oxindoles. *Angew. Chem. Int. Ed.* **52**, 1731–1734 (2013).
48. Lu, S., Poh, S. B. & Zhao, Y. Kinetic resolution of 1,1'-biaryl-2,2'-diols and amino alcohols through NHC-catalyzed atroposelective acylation. *Angew. Chem. Int. Ed.* **53**, 11041–11045 (2014).
49. Wang, M., Huang, Z., Xu, J. & Chi, Y. R. N-heterocyclic carbene-catalyzed [3 + 4] cycloaddition and kinetic resolution of azomethine imines. *J. Am. Chem. Soc.* **136**, 1214–1217 (2014).
50. Dong, S. et al. Organocatalytic kinetic resolution of sulfoximines. *J. Am. Chem. Soc.* **138**, 2166–2169 (2016).
51. Cohen, D. T., Eichman, C. C., Phillips, E. M., Zarefsky, E. R. & Scheidt, K. A. Catalytic dynamic kinetic resolutions with N-heterocyclic carbenes: asymmetric synthesis of highly substituted β-lactones. *Angew. Chem. Int. Ed.* **51**, 7309–7313 (2012).
52. Goodman, C. G., Walker, M. M. & Johnson, J. S. Enantioconvergent synthesis of functionalized γ-Butyrolactones via (3 + 2)-annulation. *J. Am. Chem. Soc.* **137**, 122–125 (2015).
53. Wu, Z., Li, F. & Wang, J. Intermolecular dynamic kinetic resolution cooperatively catalyzed by an N-heterocyclic carbene and a Lewis acid. *Angew. Chem., Int. Ed.* **54**, 1629–1633 (2015).
54. Zhao, C., Li, F. & Wang, J. N-heterocyclic carbene catalyzed dynamic kinetic resolution of pyranones. *Angew. Chem. Int. Ed.* **55**, 1820–1824 (2016).
55. Goodman, C. G. & Johnson, J. S. Dynamic kinetic asymmetric cross-benzoin additions of β-stereogenic α-keto esters. *J. Am. Chem. Soc.* **136**, 14698–14701 (2014).
56. Chen, X. et al. Carbene-catalyzed dynamic kinetic resolution of carboxylic esters. *J. Am. Chem. Soc.* **138**, 7212–7215 (2016).
57. Zhang, G. et al. Dynamic kinetic resolution enabled by intramolecular benzoin reaction: synthetic applications and mechanistic insights. *J. Am. Chem. Soc.* **138**, 7932–7938 (2016).
58. Mondal, S., Mukherjee, S., Das, T. K., Gonnade, R. & Biju, A. T. N-heterocyclic carbene-catalyzed aldol-lactonization of ketoacids via dynamic kinetic resolution. *ACS Catal.* **7**, 3995–3999 (2017).
59. DiRocco, D. A. & Rovis, T. Catalytic asymmetric α-acylation of tertiary amines mediated by a dual catalysis mode: N-heterocyclic carbene and photoredox catalysis. *J. Am. Chem. Soc.* **134**, 8094–8097 (2012).
60. Kerr, M. S., Read de Alaniz, J. & Rovis, T. A highly enantioselective catalytic intramolecular Stetter reaction. *J. Am. Chem. Soc.* **124**, 10298–10299 (2002).
61. He, M., Uc, G. J. & Bode, J. W. Chiral N-heterocyclic carbene catalyzed, enantioselective oxodiene Diels-Alder reactions with low catalyst loadings. *J. Am. Chem. Soc.* **128**, 15088–15089 (2006).
62. Kerr, M. S. & Rovis, T. Enantioselective synthesis of quaternary stereocenters via a catalytic asymmetric Stetter reaction. *J. Am. Chem. Soc.* **126**, 8876–8877 (2004).
63. Filloux, C. M., Lathrop, S. P. & Rovis, T. Multicatalytic, asymmetric Michael/Stetter reaction of salicylaldehydes and activated alkynes. *Proc. Natl Acad. Sci. USA* **107**, 20666–20671 (2010).
64. DiRocco, D. A. & Rovis, T. Catalytic asymmetric intermolecular Stetter reaction of enals with nitroalkenes: enhancement of catalytic efficiency through bifunctional additives. *J. Am. Chem. Soc.* **133**, 10402–10405 (2011).
65. Chen, X., Fang, X. & Chi, Y. *cis*-Enals in N-heterocyclic carbene-catalyzed reactions: distinct stereoselectivity and reactivity. *Chem. Sci.* **4**, 2613–2618 (2013).
66. Wen, G. et al. Stereodivergent synthesis of chromanones and flavanones via intramolecular benzoin reaction. *Org. Lett.* **18**, 3980–3983 (2016).

Acknowledgements

This work was supported by National Natural Science Foundation of China (21871260, 21502192, 21402199), the strategic priority research program of the Chinese Academy of Sciences (XDB20000000), and China Postdoctoral Science Foundation (2018M630734).

Author contributions

X.F. designed the experiment. S.P. conducted most of the experiments. X.F. and S.Y. wrote the manuscript. S.P. and S.Y. prepared the Supplementary Information. M.M. tested the single crystal structure. G.Z. helped in catalyst synthesis. W.X. and S.Y. contributed to discussions.

Additional information

Supplementary information accompanies this paper at https://doi.org/10.1038/s42004-019-0110-y.

Competing interests: The authors declare no competing interests.

Reprints and permission information is available online at http://npg.nature.com/reprintsandpermissions/

Publisher's note: Springer Nature remains neutral with regard to jurisdictional claims in published maps and institutional affiliations.